

## VERIFICATION AND VALIDATION FOR KCS TOTAL RESISTANCE

### Florentin-Daniel Popa

Romanian Navy Research Center,  
Stefanita Voda Street, No. 4  
Constanta  
“Dunarea de Jos” University of Galati,  
Faculty of Naval Architecture, Galati, Domneasca  
Street, No. 47, 800008,  
Romania,  
E-mail: florentindanielpopa@gmail.com

### Nicoleta Elena Neacșu

Romanian Navy Research Center,  
Stefanita Voda Street, No. 4  
Constanta  
“Dunarea de Jos” University of Galati,  
Faculty of Naval Architecture, Galati,  
Domneasca Street, No. 47, 800008,  
Romania,  
E-mail: mneacsu13@gmail.com

### Radu Bosoancă

“Dunarea de Jos” University of Galati,  
Faculty of Naval Architecture, Galati,  
Domneasca Street, No. 47, 800008,  
Romania,  
E-mail: radu.bosoanca@ugal.ro

### Bîlea-Pricop Andreea

Romanian Navy Research Center,  
Stefanita Voda Street, No. 4  
Constanta  
“Dunarea de Jos” University of Galati,  
Faculty of Naval Architecture, Galati,  
Domneasca Street, No. 47, 800008,  
Romania,  
E-mail: bileaandreea@yahoo.com

## ABSTRACT

*This study presents CFD simulations of the KCS model ship, focusing on ship resistance, free-surface behavior, and predictions of sinkage and trim at a Froude number of 0.26. Reynolds-Averaged Navier-Stokes (RANS) equations are solved using the  $k-\omega$  SST turbulence model. Verification and validation are carried out through a generalized Richardson Extrapolation method, following Stern's et al. [1] methodology. Results are compared with experimental data for total resistance coefficient, sinkage, trim, and wave patterns.*

**Keywords:** CFD, Richardson extrapolation, verification and validation, ship resistance.

## 1. INTRODUCTION

Accurate prediction of hydrodynamic performance is crucial in ship design, particularly for designing efficient and safe ships. Computational Fluid Dynamics has become an indispensable tool for simulating the flow around ship hulls, allowing for detailed analyses without extensive physical testing. However, the reliability of CFD simulations is significantly influenced by the quality of the

computational grid. As the number of cells in the computational grid increases, the computational time also rises significantly. Therefore, it is essential to find a grid resolution that accurately reflects physical reality without excessively increasing the number of cells and, consequently, the computational time.

In this study, the resistance of the KCS hull was simulated at a Froude number  $Fr = 0.26$ . A verification and validation study is conducted

based on a simple gener-alized Richardson Extrapolation method following the methodology discussed by Stern et al. [1]. Total resistance coefficient, sinkage, trim, and wave patterns were compared with experimental results provided by NMRI [2].



Fig. 1 Hull geometry

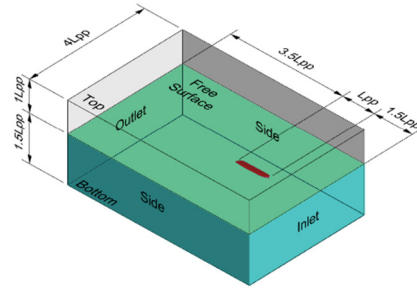


Fig. 2 Domain topology and boundary conditions

## 2. GEOMETRY AND CONDITIONS

The KRISO Container Ship (KCS) hull was selected for the present research, with all computations performed at a 1/42 model scale. The main particulars of the KCS hull are presented in Table 1.

Table 1 Main particulars

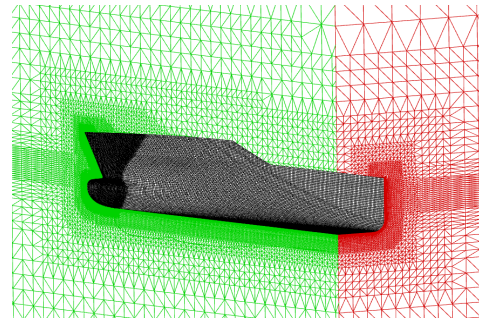
Main particular	Scale	
	1/1	1/42
$L_{BP}$ [m]	230	5.476
B [m]	32.2	0.766
D [m]	19	0.452
T [m]	10.8	0.257
$\nabla$ (m <sup>3</sup> )	52030	0.702
$v$ [Kn]	24	3.703
$C_B$	0.6505	0.6505
$S_W$ [m <sup>2</sup> ]	9424	5.342
Rudder type	Horn	Horn
Rudder profile type	NACA0019	NACA0019
$S_R$ (m)	115	0.065

The computational domain consists of a rectangular prism with the following dimensions relative to the Length Between Perpendiculars ( $L_{BP}$ ):

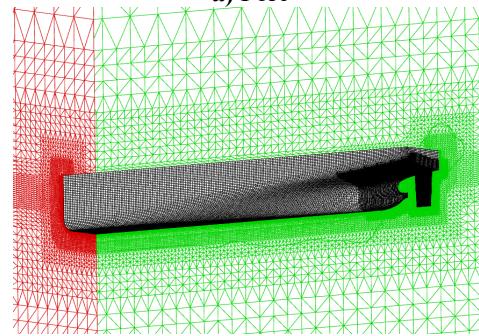
- In the x direction:  $6 L_{BP}$
- In the y direction:  $4 L_{BP}$
- In the z direction:  $2.5 L_{BP}$

Figure 2 presents the computational domain and boundary conditions.

The upstream boundary is positioned  $1.5 L_{BP}$  from the fore perpendicular, while the downstream boundary is located  $3.5 L_{BP}$  from the aft perpendicular. The side boundaries are set at  $2 L_{BP}$  from the ship's centerline, with the upper and lower boundaries positioned  $1 L_{BP}$  above and  $1.5 L_{BP}$  below the free surface, which is aligned with the ship's design draft. A wall function is applied near the hull and rudder calibrated for a non-dimensional wall distance of  $y^+ = 50$ . Slip condition is applied for the deck.



a) Fore



b) Aft

Fig. 3 Fine grid

The computational grids were generated using the HEXPRESS automatic grid generator included in the FINE™/MARINE software, based on the imported hull geometry. Figure 3 illustrates the fine mesh generated for the computations of the flow around the hull, including a simplified rudder geometry.

The numerical simulations were conducted using the ISIS-CFD solver, part of the FINE™/MARINE software suite provided by CADENCE. This solver employs the finite volume method to discretize the transport equations and solve the Reynolds-Averaged Navier Stokes Equations (RANSE). To accurately capture the air–water interface, the free surface was modeled using the Volume of Fluid (VOF) method, utilizing the Blended Interface Capturing Scheme with Reconstruction (BRICS). Turbulence closure was achieved through the Shear Stress Transport (SST)  $k-\omega$  model.

Quasi-steady computations were carried out for an inflow velocity corresponding to  $Fr = 0.26$  with trim and sinkage degrees of freedom set to be solved. All simulations were run for a total of 30 seconds, with convergence achieved after 25 seconds.

### 3. RESULTS AND DISCUSSIONS

First, a verification and validation process was conducted following the methodology described in [1], aimed at evaluating the discretization errors due to grid size and time step selection. Three different grid resolutions were generated, referred to as coarse (S3), medium (S2), and fine (S1). The S3 grid contained approximately  $2.22 \times 10^6$  cells, the S2 grid had  $3.34 \times 10^6$  cells, and the S1 grid included  $4.66 \times 10^6$  cells.

For the time step convergence study, simulations were carried out using the medium grid. Three sets of time steps - coarse, medium, and fine - were tested, based on a refinement ratio  $r_T = 1.5$ , without exceeding the time step recommended by the ITTC,  $\Delta t = 0.005 \times L_{BP}/U$ . The coarse time step was set to 0.015, the medium time step to 0.01, and

the fine time step to 0.00667. All grid-related simulations were performed using the medium time step, and all time step-related simulations were conducted using the medium grid. Figures 3, 4, and 5 show the variation of the relative error compared to EFD for grid convergence, in relation to the number of cells ( $N_c$ ).  $\epsilon_{C_T}$  represents relative error for the Total Resistance Coefficient ( $C_T$ ) while  $\epsilon_\sigma$  and  $\epsilon_\tau$  represents relative error for sinkage ( $\sigma$ ) and trim ( $\tau$ ).

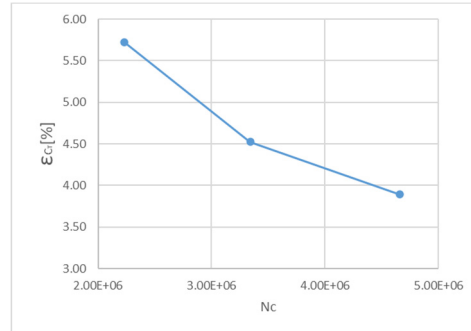


Fig. 3  $\epsilon_{C_T}$  vs  $N_c$

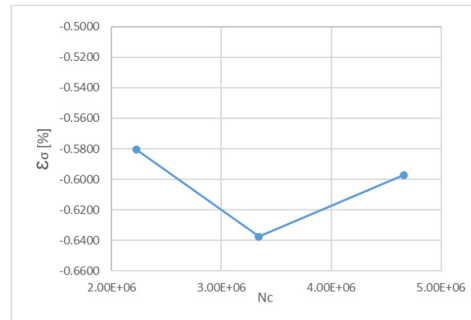


Fig. 4  $\epsilon_\sigma$  vs  $N_c$

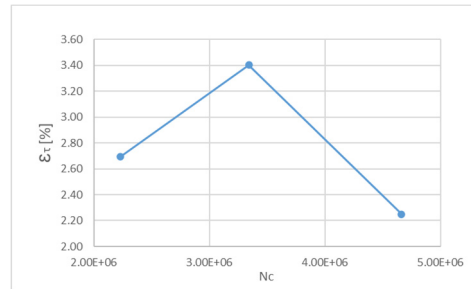


Fig. 5  $\epsilon_\tau$  vs  $N_c$

For  $C_T$ , as the grill becomes more refined, the relative error compared to EFD decreases asymptotically indicating monotonic convergence. However, the same cannot be said for sinkage and trim which do not show monotonic convergence. Another simulation with a further refined grid is required to determine if the value converges. Despite this, the maximum error for  $\sigma$  is relatively low, around 0.64%, and for  $\tau$ , it is around 3.4%. These low error values indicate a good agreement with the EFD results.

Figures 6, 7, and 8 illustrate the variation in error relative to the EFD results with respect to the time step ( $\Delta t$ ).

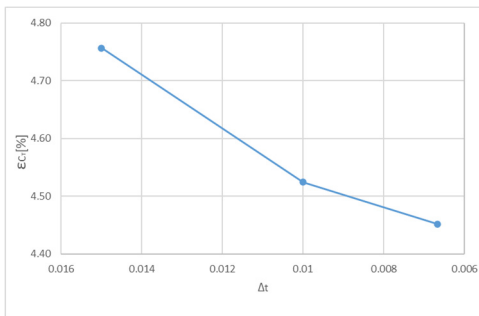


Fig. 6  $\varepsilon_{C_T}$  vs  $\Delta t$

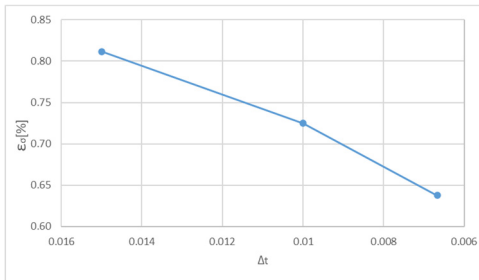


Fig. 7  $\varepsilon_{\sigma}$  vs  $\Delta t$

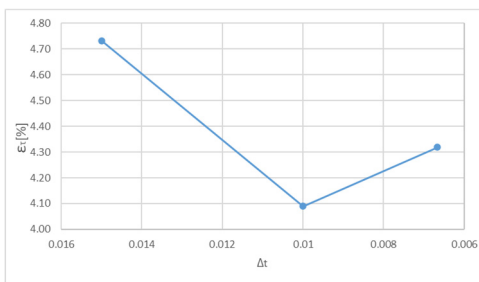


Fig. 8  $\varepsilon_{\tau}$  vs  $\Delta t$

Similar to the grid convergence test, only  $C_T$  show monotonic convergence in the time step convergence study. For sinkage and trim, the errors do not exhibit monotonic convergence. Despite this non-monotonic behavior, the overall error values remain low, indicating that the solution remains within a reasonable range of accuracy even with var-ying time step sizes.

Table 2 presents a detailed comparison between numerical solutions for the  $C_T$ ,  $\sigma$  and  $\tau$  and experimental data provided by NMRI [2]. The values labeled GS are derived from the solutions corresponding to different grid sizes, while the values labeled TS are obtained from the solutions corresponding to different time step sizes.

Table 2 Results

EFD		$C_T \times 10^3$	$\sigma/L_{pp} \times 10^2$	$\tau$ [°]
CFD		3.711	-0.1915203	-0.169
S3	GS	3.923	-0.1904087	-0.1736
	$\varepsilon$ [%]	5.72	0.58	2.69
	TS	3.888	-0.1899661	-0.1743
	$\varepsilon$ [%]	4.76	0.81	4.73
S2	GS	3.879	-0.1902995	-0.1747
	$\varepsilon$ [%]	4.52	0.64	3.40
	TS	3.879	-0.1901317	-0.1736
	$\varepsilon$ [%]	4.52	0.73	4.09
S1	GS	3.855	-0.1903769	-0.1728
	$\varepsilon$ [%]	3.89	0.60	2.25
	TS	3.876	-0.1902992	-0.1739
	$\varepsilon$ [%]	4.45	0.64	4.32

The computed errors range from 0.58% to 5.72%, independent of grid or time step size. The resulting grid uncertainty and time step uncertainty are presented in Table 3.

Table 3 Uncertainty analysis

Grid uncertainty		Time step uncertainty	
Parameter	Value	Parameter	Value
$r_G$	1.4	$r_T$	1.5
$\varepsilon_{21} \% S_1$	0.6	$\varepsilon_{21} \% S_1$	0.069
$P_g/P_{g,th}$	0.96	$P_T/P_{T,th}$	1.44
$U_g \% S_1$	0.68	$U_T \% S_1$	0.031

The validation uncertainty is expressed as  $U_V = \sqrt{U_G^2 + U_T^2 + U_D^2}$  where  $U_G$  represents grid uncertainty,  $U_T$  represents time step

uncertainty and  $U_D$  is experimental uncertainty.  $r_c$  is the grid refinement

In our case  $U_V = 1.21\%$  indicating that the model does not meet validation criteria using this method. However, since both  $U_g$  and  $U_T$  are less than 1%, this suggests that the model is independent of grid and time step resolution. This means that indifferent of what time step or grid size is chosen, the final result doesn't change significantly.

Next, a comparison of the free surface topology between the EFD and CFD results is presented. Figure 9 shows the comparison between the computed and measured wave profiles along the ship hull.

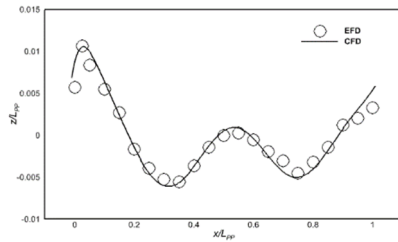


Fig. 9 Wave elevation on hull comparison with EFD

The CFD results closely follow the experimental data across most of the profile, accurately capturing key wave characteristics. However, slight deviations are evident at certain positions, particularly in regions with rapid changes in wave elevation, such as near the bow and aft of the ship. These differences suggest that the CFD model may slightly under or over-predict wave elevation in these areas.

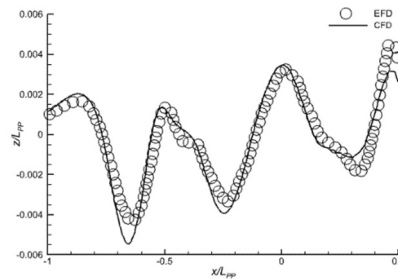


Fig. 10 Wave elevation cut at  $y/LBP=0.1509$  comparison with EFD

A likely cause of this variation is that the computational grid resolution does not adhere to the theoretical requirement of at least 50 cells per wavelength in both the x and y directions [3].

The comparison from Figure 10 more clearly highlights the impact of the insufficient grid resolution on the wave area. The CFD results show noticeable discrepancies from the experimental data, especially in regions where wave height changes rapidly. These variations are more pronounced here compared to the previous case, reinforcing that the lack of sufficient cells per wavelength, below the theoretical minimum, causes the CFD to under- or over-predict wave elevation. The deviations seen in this comparison emphasize the critical importance of ensuring proper grid resolution for accurately capturing wave phenomena. Figure 11 presents a comparison for free surface topology between CFD and EFD data from Kim et al. [4].

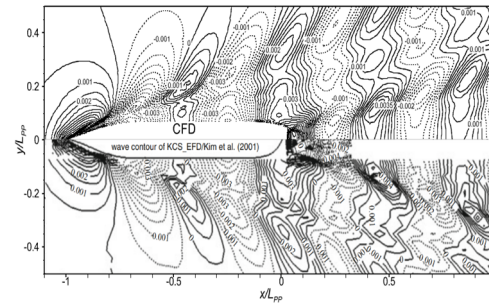
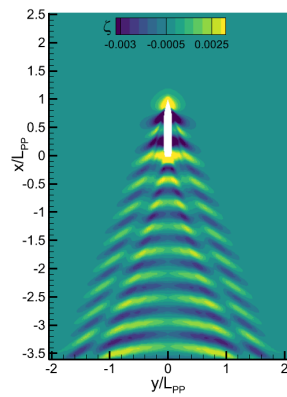
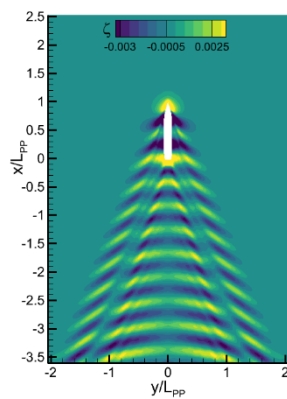


Fig. 11 Free surface topology comparison with EFD [4]

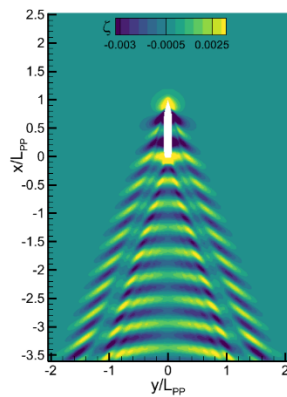
The overall shape of the wave pattern appears consistent with experimental data, with smooth contour lines indicating regions of gradual wave elevation changes, and denser contours in areas where the wave steepness increases. The CFD simulation seems to effectively replicate the bow wave and the wake. Although slight discrepancies could be seen in some regions with higher complexity, which most likely arise from insufficient grid resolution. Figure 12 presents a comparison of the free surface topology for all three grid resolutions.



a) Coarse



b) Medium



c) Fine

**Fig. 12** Free surface topology

Despite some minor variations, all grid resolutions: coarse, medium, and fine exhibit a strong alignment in the predicted wave patterns. While the coarse grid successfully reproduces the overall wave structure, the medium and fine grids progressively reveal more detailed wave features. The fine grid provides the most accurate depiction of wave elevations, capturing subtle variations that are less distinct in coarser grids.

#### 4. CONCLUSIONS

The verification and validation study conducted on the KCS model using CFD simulations demonstrated a reasonable agreement between computational and experimental results for ship resistance, with an error range from 0.58% to 5.72%. The study was performed at a Froude number of 0.26. Although some deviations were noted, the overall agreement with experimental data confirms the capability of the CFD model. Some parameters, such as sinkage and trim, exhibited non-monotonic convergence behavior suggesting that another simulation with a finer grid is needed for further validation.

The free-surface flow predictions showed good alignment with experimental results, with minor phase shifts and slight variations in wave amplitude at critical points, emphasizing the importance of grid resolution in accurately capturing these phenomena.

Overall, the CFD results prove effective in ship resistance computations and free-surface prediction, although further investigations, particularly grid refinement, are recommended. These improvements would enhance the reliability of future simulations, especially if applied to more complex configurations, such as fully appended hull resistance computations.

#### Acknowledgments

The research was supported by the Research Centre of the Faculty of Naval Architecture, "Dunarea de Jos" University of Galati, which is greatly acknowledged.

## REFERENCES

- [1] F. Stern, R. V. Wilson, H. W. Coleman, and E. G. Paterson, "Verification and Validation of CFD Simulations," US Dept of the Navy, Fort Belvoir, VA, Sep. 1999. doi: 10.21236/ada458015.
- [2] L. Larsson, F. Stern, and M. Visonneau, Eds., *Numerical Ship Hydrodynamics: An assessment of the Gothenburg 2010 Workshop*. Dordrecht: Springer Netherlands, 2014. doi: 10.1007/978-94-007-7189-5.
- [3] A. Lungu, *Modelari numerice in hidrodinamica - Grile de discretizare*, vol. 1, 1 vols. Editura Tehnica, 2000.
- [4] W. J. Kim, S. H. Van, and D. H. Kim, "Measurement of flows around modern commercial ship models," *Exp. Fluids*, vol. 31, no. 5, pp. 567–578, Nov. 2001, doi: 10.1007/s003480100332.
- [5] A. Bekhit and A. Lungu, "Verification and validation study for the total ship resistance of the DTMB 5415 ship model," *Ann. "DUNAREA JOS" Univ. GALATI FASCICLE XI – Shipbuild.*, vol. 40.
- [6] A. Lungu, "Numerical Simulation of the Resistance and Self-Propulsion Model Tests1," *J. Offshore Mech. Arct. Eng.*, vol. 142, no. 2, Apr. 2020, doi: 10.1115/1.4045332.
- [7] V. Bertram, *Practical ship hydrodynamics*. Oxford ; Boston: Butterworth-Heinemann, 2000.
- [8] "ITTC - Recommended Procedures and Guidelines - 7.5-03-02-01."
- [9] "ITTC - Recommended Procedures and Guidelines - 7.5-03-02-03."

**Paper received on October 1<sup>st</sup>, 2024**

